

Robot Localization Using a Learned Keypoint Detector and Descriptor with a Floor Camera and a Feature Rich Industrial Floor

Piet Brömmel², Dominik Brämer^(✉)¹, Oliver Urbann² and Diana Kleingarn¹

¹ Robotics Research Institute, Section Information Technology,
TU Dortmund University, 44227 Dortmund, Germany

² Fraunhofer IML,
Joseph-von-Fraunhofer-Str. 2-4, Dortmund, Germany
`dominik.braemer@tu-dortmund.de`

Abstract. The localization of moving robots depends on the availability of good features from the environment. Sensor systems like Lidar are popular, but unique features can also be extracted from images of the ground. This work presents the Keypoint Localization Framework (KOALA), which utilizes deep neural networks that extract sufficient features from an industrial floor for accurate localization without having readable markers. For this purpose, we use a floor covering that can be produced as cheaply as common industrial floors. Although we do not use any filtering, prior, or temporal information, we can estimate our position in 75.7% of all images with a mean position error of 2 cm and a rotation error of 2.4%. Thus, the robot kidnapping problem can be solved with high precision in every frame, even while the robot is moving. Furthermore, we show that our framework with our detector and descriptor combination is able to outperform comparable approaches.

Keywords: Robot localization · Kidnapped robot problem

1 Introduction

Indoor localization is crucial for autonomous mobile robots, making it a key research topic and of significant commercial interest. The current position is essential for various applications, leading to multiple approaches. GPS is a precise and widely known solution that is unsuitable for indoor applications. Ultra-wideband requires expensive hardware to be mounted in the whole location. As a result, these methods are rarely used in mobile robots.

A popular approach is using light detection and ranging (Lidar) sensors together with a simultaneous localization and mapping (SLAM) method. The price range for these sensors vary widely and with it the range of capabilities, e.g., the maximum measurable distance and speed of rotation.

Another popular class of methods is the feature detection of the environment with cameras. These can be QR codes stuck on the floor, ceiling, or other artificial

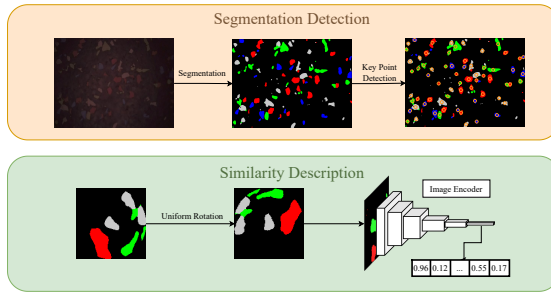


Fig. 1. A conceptual overview of our segmentation detector and similarity descriptor. Upper: Raw image segmented into an RGBW mask with detected keypoints. Lower: Keypoint patches are rotated uniformly and encoded into latent vectors by a pretrained encoder.

features placed in the environment. It is also possible to detect features that are naturally present.

However, sensing static features in dynamic environments with many moving objects (e.g., other robots or people) is generally challenging. Therefore, a typical viewing direction for cameras is towards the ceiling [23]. Occlusions and the large distance to the roof can be tricky and make it hard to detect smaller features.

In this paper, we investigate the possibility of mounting the camera beneath the robot, allowing for a close-up view of the ground. This eliminates occlusions, particularly from moving objects, and ensures uniform illumination. For this reason, we present a floor image localization framework based on a custom keypoint detector and descriptor.

Possible features to be detected are QR codes for driving predefined paths [20]. A dense mesh of QR codes is needed to use them on the ground to localize beyond predefined paths.

At the other extreme are popular floor coverings such as concrete or asphalt [3]. In this work, we choose a trade-off between these two poles and use industrial flooring typical for robotics. In its production, black granulate is used as a base color mixed with red, green, blue, and white colored granulates. This creates a random red, green, blue, and white (RGBW) pattern on a black background that is clearly visible, see Figure 4. We use this pattern for localization with a preceding phase for mapping.

2 Related Work

As mentioned above, methods for simultaneous localization and mapping (SLAM) based on cameras or laser scanners are very popular [15,16]. Other examples of localization methods use cameras pointed at the ceiling as proposed by Hwang et al. and Chen et al. [2,11], who also confirm the disadvantages mentioned in section 1.

A few publications already address the application of ground cameras. In general, it can be shown that methods like SIFT and CenSure are well suited to extract features from patterns on the ground [18].

Kozak et al. propose a method with commercially available hardware to perform map-based localization using a ground-facing camera [12]. For their best localization results, they use a combination of CenSure and SIFT as feature detector and descriptor, but they operate in productive use a combination of CenSure and ORB for a faster execution time. They apply it to asphalt and report a good lateral accuracy within 2 cm, but without exact numbers due to missing ground truth values. The system proposed by Kozak et al. depends on previous positions to deliver a correct localization through an extended Kalman filter. Therefore, they need an initial starting position and cannot solve the robot kidnapping problem.

Similarly, Zhang et al. and Schmid et al. have developed a high-precision localization that works on different floor types, such as asphalt, concrete, tiles, and carpet [19,24]. They use SIFT as a feature detector and SIFT or LATCH as a descriptor for their best localization results. Instead of position prediction, they perform image retrieval for evaluation, due to missing ground truth data.

In particular, CNN encoders, as an approach from the field of machine learning, are a popular method to learn a compressed representation for a set of data [26]. This representation can be utilized to find similar images [6].

SIFT is particularly successful because of Lowe’s matching criterion. In order to make this advantage available for deep neural networks, Mishchuk et al. propose a loss that maximizes the distance between the closest positive and closest negative example [14].



Fig. 2. Overview of the experimentation hall showing the motion capture system and the industrial floor.



Fig. 3. Modified DJI Robomaster S1 with a floor camera and markers for the motion capture system.

Zhang et al. utilize this to apply an autoencoder that generates descriptions of selected parts (keypoints) of an image. They apply this method to reidentify images of textured floors [25]. By combining this with a SIFT descriptor, they motivate the application as a localization method. However, this application is only briefly introduced, and the localization error against a ground truth position is not evaluated.

In contrast, Chen et al. [3] present a complete localization pipeline and report localization errors on various floors: a few millimeters on floors with visible lines

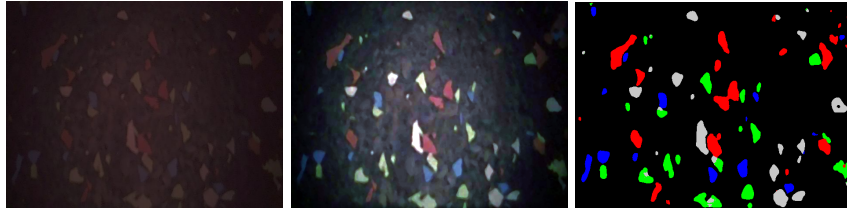


Fig. 4. Left, a raw $4.95\text{ cm} \times 2.80\text{ cm}$ floor image with RGBW pattern. The same image brightened and contrasted for improved clarity in the middle, and the segmentation mask of the image on the right.

(e.g., tiled floors) and 10 cm up to 13 cm on general floors. However, as lines cannot be identified uniquely and sometimes no line is visible, the solution for tiled floors is combined with an extended Kalman filter, and in some cases, a different system has to provide an initial localization. Furthermore, rotation localization error is not evaluated as no ground truth data exists.

2.1 Contribution

As can be seen in the related research, localization on general soils still poses a challenge. Therefore, this paper proposes a localization framework that

- uses an industrial floor made of random colored plastic granulate for position prediction,
- uses a custom keypoint detector and descriptor,
- provides a localization with a mean distance error of around 2 cm,
- does not use temporal information,
- is evaluated utilizing a motion capture system.

Furthermore, we use our dataset with ground truth positions consisting of 1.2 million images (280 GB) described in section 3 to train, test and evaluate our approach. We also use it to benchmark our approach against other comparable approaches of Kozak et al. [12] and Zhang et al. [24] that have not been studied with this accuracy before.

2.2 Structure

We begin by introducing the dataset of overlapping floor images in section 3 which covers an area of 144 m^2 , and the evaluation runs. In section 4, we present our approach for the detector and descriptor, along with our localization framework (KOALA). This framework includes two main components: map creation and position estimation, both of which are explained in section 4. Finally, in section 5, we evaluate the performance of KOALA using our detector and descriptor compared to other feature extraction methods discussed in section 2.

3 Dataset

The dataset for this work was recorded in our lab due to a lack of available datasets. A thorough search showed that only Zhang et al. published a dataset with different floor types. However, the ground truth position information were not part of this dataset [24]. To provide ground-truth position information for each image in our dataset, we use a motion capture system. Figure 2 shows an overview of the hall, the motion capture system, and the area covered with the industrial floor.

We use cameras from the company Vicon, model V5, V8, and V16, for which the robot is equipped with markers, see Figure 3. The images of the ground are captured at a frequency of 60 Hz and the position of the robot on the field at a frequency of 200 Hz. We synchronize the images and positions to gain our training and evaluation dataset with a precision of 0.5 cm.

The images are recorded using a Raspberry Pi Camera Module 2 and an LED ring. Lens distortion correction is applied to every image. The camera captures an area of $4.95 \text{ cm} \times 2.80 \text{ cm}$ with $632 \text{ px} \times 480 \text{ px}$. An example image of the floor can be seen in Figure 4.

The dataset consists of 36 mapping runs of $2 \text{ m} \times 2 \text{ m}$ covering 144 m^2 and 12 evaluation runs. The evaluation runs are split into 4 groups covering 4 m^2 , 36 m^2 and 144 m^2 . The mapping runs are captured with a robot speed of 0.2 m/s for more overlapping mapping images. In contrast, the evaluation runs are captured with 0.3 m/s , which was the maximum travel speed without a high degree of motion blur.

4 System Design

This section presents a custom Segmentation Detector (SEG) and Similarity Descriptor (SIM). Furthermore, we propose our localization framework consisting of a map creation and position estimation step.

4.1 Detector

Relevant features for this floor are red, green, blue, and white color blobs, which can be obscured by sensor noise and lighting conditions (Figure 4). To filter this noise, our keypoint detector first employs a U-Net Xception-style segmentation model that learns a mask for the four colors, as this architecture could achieve good results with a low runtime [5,17]. Given the local nature of these features, we reduce the network to two stages with an 8-filter size to boost speed and generalization. We manually annotated 20 images from our dataset (16 for training, 4 for validation) and used flip, crop, shear, translate, and rotate augmentations to extend our training and validation images. Training for 4000 iterations with a batch size of 64 yielded a final sparse categorical cross-entropy validation loss of 0.072.

In the second step, color blobs are extracted from the segmented image using a connected component labeling algorithm based on Fiorio et al. [8,22]. The center of a color blob is used as a keypoint if

1. the center is 64 px away from the image border,
2. the area of the color blobs contains more than 150 px and
3. there are at least 500 colored pixel in a radius of 64 px around the center.

4.2 Descriptor

We extract a rotation-invariant descriptor from a circular region with a radius of 64 px around each keypoint by first rotating the image and then encoding it with a CNN. To achieve uniform rotation, we approximate each color blob with an ellipse and align the patch according to its major axis, ensuring the upper half contains more colored pixels—a necessary step given CNNs’ limited rotation invariance [10].

We train our network with supervised contrastive loss [13] on patches from the same and different keypoints. The CNN is composed of two convolution blocks with filter counts of 8 and 16. Each block starts with two convolution layers with the same number of filters, a kernel size of three, and a Rectified Linear Unit (ReLU) activation function and ends with a max-pooling layer to downsample the width and height of the input. After the convolutional layers, we flatten the output and use a dense layer with size 30 and an L2 normalization as our final output. For training, we use the Multi-Similarity Loss [1] with the Adam optimizer and a learning rate of 0.0001. We train the model for 15000 steps with a batch size of 4096 and early stopping to prevent overfitting. The model weights with the smallest validation loss over the entire training run are used as the final weights of our model. For the implementation, we use the Tensorflow Similarity library [21].

The training dataset is generated by clustering keypoint patches (from another descriptor) that correspond to the same floor feature. Clusters with at least four members (as detailed in subsection 4.3) yield four uniformly sampled images per cluster. An overview of the Segmentation Detector (SEG) and Similarity Descriptor (SIM) is shown in Figure 1.

4.3 Map Creation

We create a map database with keypoint descriptions and their position from the mapping runs. The database is created with the following steps:

- Image gathering with ground truth position.
- Outlier removal of ground truth positions.
- Process each image with a keypoint detection and description algorithm.
- Calculate the global position of each keypoint.
- Clustering and merging of keypoints.
- Storing and indexing of the descriptions in a database.

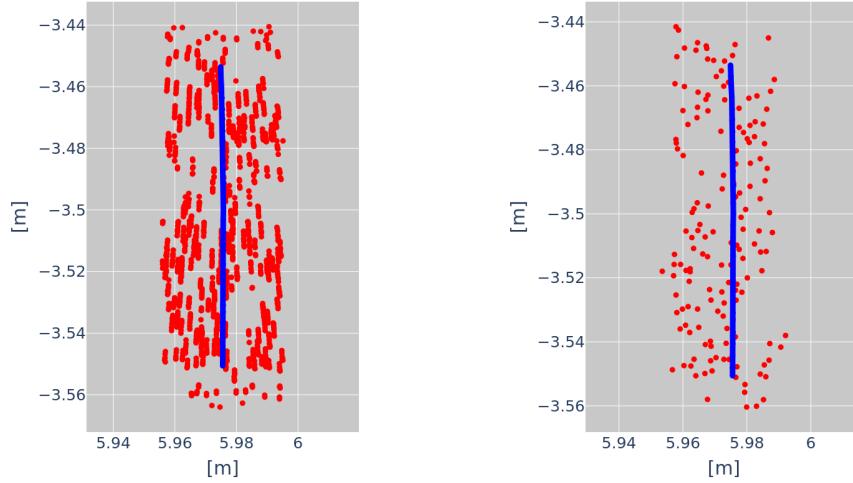


Fig. 5. Keypoints extracted from a run before clustering (left) and after (right).

The floor images are captured with our robot as described in section 3.

Due to noise in the motion capture system, outliers are removed using a sliding window. The window moves over the ground truth positions along the recorded track. In each window, we compute the mean value μ and the standard deviation σ of the positions. A new position p_I is discarded if the deviation $d = |\mu - p_I|$ of this position from σ exceeds the value $\alpha \cdot \sigma$ with a manually selected α of 0.8.

Clustering is required as each image is processed with a keypoint detector and descriptor to determine global keypoint positions from the image’s global coordinates and pixel locations. Given the zigzag capture pattern and overlapping images, the same color blob is often mapped multiple times.

For clustering, we iterate through keypoints and select those within 0.5 cm of each candidate, excluding keypoints from the same image or those already labeled. We then compute the cosine distance between descriptors and define a cluster as at least four keypoints with a cosine distance below 0.1. This approach is a simplified variant of DBSCAN [7] that avoids transitive expansion for arbitrary shapes (Figure 5).

4.4 Position Estimation

The position estimation predicts the position of an image independently without any prior information about previous positions and thus solves the kidnapping robot problem with every prediction. An overview of the framework is shown in Figure 6.

For each image, keypoints and descriptors are obtained as in the map-creation process, and an approximate k-nearest neighbor search using TensorFlow Similarity [1] retrieves 20 comparable keypoints from the map database. Despite many spurious matches, the location with the highest match density (the mode)

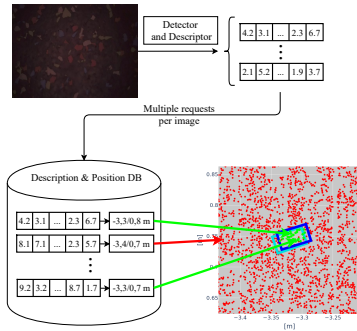


Fig. 6. Pipeline for position estimation of a given image.

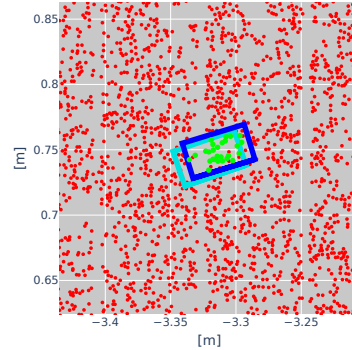


Fig. 7. Database map: blue rectangle: estimated position, cyan: ground truth; red dots indicate stored keypoints, green dots show queried matches.

likely corresponds to the true position; hence, the keypoint with the most nearby matches is selected.

Subsequently, the optimal Euclidean transformation aligning the image keypoints with their map counterparts is computed using the filtered matches. RANSAC is utilized to obtain the optimal transformation from the noisy data since some matches may still be mismatched [4,9]. For RANSAC, we utilize a minimum sample size of three, a residual threshold of 0.002, and a maximum of 100 trials. This transformation yields the predicted image position; if too few filtered matches exist or RANSAC fails, no prediction is made. Figure 7 illustrates a successful localization.

5 Evaluation

With the evaluation, we pursue the following goals: we evaluate the KOALA framework with various combinations of detectors and descriptors, as well as our Segmentation Detector and Similarity Descriptor, and we test our dataset of the feature-rich industrial floor. We benchmark against baselines inspired by Kozak et al. [12] and Zhang et al. [24].

The framework is evaluated using four evaluation runs for each of the three areas of the dataset with sizes of 4 m^2 , 36 m^2 , and 144 m^2 .

We use multiple metrics to measure the quality of the KOALA framework. For the prediction success rate (PSR), we consider the localization a success if the localization framework does not fail. For the true success rate (TSR), a successful localization is defined as the predicted position being no more than 10 cm and 20 degree away from the ground truth position and rotation. The mean distance and the mean rotational delta are calculated for each successful localization between the predicted and ground truth positions. To obtain fewer false-positive predictions, it is also crucial for the PSR to be near the TSR.

We use SIFT and CenSure combinations as baseline detector/descriptor approaches, as they have shown strong performance in this field [12,24]. To eval-

uate KOALA, we compare these baseline approaches with our learned detector/descriptor as an alternative.

In addition, we tested SIFT as a detector in combination with our descriptor to see how well this combination works on our dataset.

For the evaluation of CenSure and SIFT, we primarily rely on the default parameters provided by the OpenCV implementation. However, to ensure consistency in the number of detected features corresponding to the colored blobs in the image, we adjust specific parameters. For CenSure, the *responseThreshold* is set to 9, while for SIFT, *nfeatures* is adjusted to 70, and *contrastThreshold* is set to 0.03.

Table 1. Success rate, mean position and angle errors of multiple detector and descriptor combinations for the 144 m² area.

Method	True Success Rate	Predicted Success Rate	Position Error	Angle Error
SIFT-SIFT	32.7 %	34.3 %	0.017 m	2.8°
CenSure-SIFT	7.6 %	12.1 %	0.004 m	2.6°
SIFT-SIM-3	63.0 %	69.4 %	0.019 m	2.8°
SEG-SIM-1	64.3 %	67.4 %	0.019 m	2.4°
SEG-SIM-2	73.4 %	76.4 %	0.019 m	2.4°
SEG-SIM-3	75.7 %	78.0 %	0.020 m	2.4°

When training the Similarity Descriptor, it is important to use a good descriptor to get a better training dataset using clustering. Therefore, we train three Similarity Descriptors iteratively, with SIFT generating the training dataset for SIM-1, SIM-1 generating the training dataset for SIM-2, and SIM-2 generating the training dataset for SIM-3.

The results of the detector and descriptor combinations on all three areas can be seen in Figure 8 and for the biggest area in Table 1.

According to Figure 8, the general performance of CenSure-SIFT and SEG-SIFT is unsatisfying. This may be because many keypoints are in the middle of the color blobs, and SIFT does not seem to work well there since it only references a small area around each keypoint to generate its description.

It can also be seen in Table 1 that the true success rate performance increases with training multiple Similarity Descriptors iteratively from 64.3 % to 75.7 %. Our learned approach also outperforms SIFT by a significant margin. The results also show a good mean position and angle error for all tested methods.

Figure 9 shows the ground truth and predicted position of all images in an evaluation run in the 36 m² area using SEG-SIM-3.

Execution time is another essential metric for robot localization. The timings were measured using an Nvidia Jetson Xavier NX board installed on the robot, with no further improvements to our framework, detector, or descriptor. SIFT-SIFT takes 0.59 s, and SEG-SIM-3 takes 1.05 s to estimate the position of one image. Another distinction between the SIFT descriptor and our Similarity Descriptor is that our approach uses a smaller description dimension of 30, while

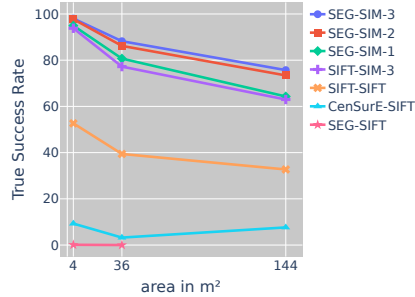


Fig. 8. Evaluation of different detector and descriptor combinations for an area of 4 m^2 , 36 m^2 and 144 m^2 .

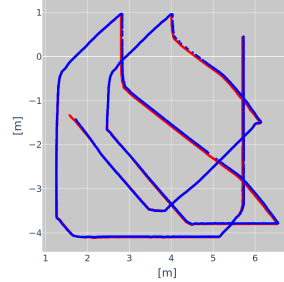


Fig. 9. Trajectory of ground truth (red) and predicted (blue) robot positions on an evaluation run in the 36 m^2 area using SEG-SIM-3.

SIFT uses 128. This means that our descriptions are about four times smaller and therefore take up less space in the map database.

We conducted an analysis to evaluate the impact of specific components of our descriptor on position estimation performance. This investigation aims to assess the generalization capability of our descriptor while simultaneously addressing the timing overhead associated with the unified rotation algorithm. Therefore we tested if the CNN encoder is able to learn rotation-invariant descriptions instead of using our unified rotation algorithm. To achieve this, we have trained the CNN encoder with randomly rotating patches showing the same keypoints.

We also trained a CNN encoder to work with RGB instead of segmentation mask patches. Our proposed change allows our descriptor to work with other detectors without generating a segmentation mask.

Ablation Study The result of our ablation study is shown in Table 2. Our Similarity Descriptor can become rotation invariant at the expense of the true success rate.

The generalization to RGB images works quite well, performing almost as well as SEG-SIM-3 with a learned rotation. Both variants still significantly outperform SIFT-SIFT.

Table 2. Evaluation of the 144 m^2 run with SEG-SIM-3 testing learned rotation invariance and RGB patches.

Method	Learned Rotation	RGB	True Success Rate
SEG-SIM-3	No	No	75.7 %
SEG-SIM-3	Yes	No	61.4 %
SEG-SIM-3	Yes	Yes	56.6 %

6 Conclusion and Future Work

This paper shows the flexibility of our framework using different detector and descriptor combinations and that it can be used for ground localization of huge

areas using the suitable detector and descriptor combination for the used floor. We show that an industrial floor where colored granules were used for production instead of single-colored granules works well for scaled up ground localization. It should be mentioned, that for localization, we use small images where each image only covers a fraction of $9.625 \cdot 10^{-6}$ of the 144 m^2 area.

Even with such a small image, it is possible with the framework and our proposed detector and descriptor to localize with an accuracy of 2 cm in 3 out of 4 cases. The Segmentation Detector proposed by us, which is tailor-made for this floor, in combination with our Similarity Descriptor, outperforms other detector/descriptor combinations. Still, it has been shown that even these can achieve good results in variety with our framework.

To be able to use the framework productively in logistic halls, it makes sense to extend our system to a SLAM-like algorithm to eliminate the need for a motion tracking system to create a global map.

Furthermore, it is desirable to reduce the localization execution time to make it real-time usable and to make our detector usable for other floors as well.

References

1. Bursztein, E., Long, J., Lin, S., Vallis, O., Chollet, F.: Tensorflow similarity: A usable, high-performance metric learning library. Fixme (2021)
2. Chen, X., Jia, Y.: Indoor localization for mobile robots using lampshade corners as landmarks: Visual system calibration, feature extraction and experiments. *International Journal of Control, Automation and Systems* **12**(6), 1313–1322 (2014)
3. Chen, X., Vempati, A.S., Beardsley, P.: Streetmap-mapping and localization on ground planes using a downward facing camera. In: 2018 IEEE/RSJ International Conference on Intelligent Robots and Systems (IROS). pp. 1672–1679. IEEE (2018)
4. Choi, S., Kim, T., Yu, W.: Performance evaluation of ransac family. *Journal of Computer Vision* **24**(3), 271–300 (1997)
5. Chollet, F.: Xception: Deep learning with depthwise separable convolutions (2017)
6. En, S., Crémilleux, B., Jurie, F.: Unsupervised deep hashing with stacked convolutional autoencoders. In: 2017 IEEE International Conference on Image Processing (ICIP). pp. 3420–3424. IEEE (2017)
7. Ester, M., Kriegel, H., Sander, J., Xu, X.: A density-based algorithm for discovering clusters in large spatial databases with noise. In: Simoudis, E., Han, J., Fayyad, U.M. (eds.) *Proceedings of the Second International Conference on Knowledge Discovery and Data Mining (KDD-96)*, Portland, Oregon, USA. pp. 226–231. AAAI Press (1996), <http://www.aaai.org/Library/KDD/1996/kdd96-037.php>
8. Fiorio, C., Gustedt, J.: Two linear time union-find strategies for image processing. *Theoretical Computer Science* **154**(2), 165–181 (1996)
9. Fischler, M.A., Bolles, R.C.: Random sample consensus: a paradigm for model fitting with applications to image analysis and automated cartography. *Communications of the ACM* **24**(6), 381–395 (1981)
10. Goodfellow, I., Lee, H., Le, Q., Saxe, A., Ng, A.: Measuring invariances in deep networks. *Advances in neural information processing systems* **22**, 646–654 (2009)
11. Hwang, S.Y., Song, J.B.: Monocular vision-based global localization using position and orientation of ceiling features. In: 2013 IEEE International Conference on Robotics and Automation. pp. 3785–3790 (2013). <https://doi.org/10.1109/ICRA.2013.6631109>

12. Kozak, K., Alban, M.: Ranger: A ground-facing camera-based localization system for ground vehicles. In: 2016 IEEE/ION Position, Location and Navigation Symposium (PLANS). pp. 170–178. IEEE (2016)
13. Kulis, B., et al.: Metric learning: A survey. *Foundations and Trends® in Machine Learning* **5**(4), 287–364 (2013)
14. Mishchuk, A., Mishkin, D., Radenovic, F., Matas, J.: Working hard to know your neighbor’s margins: Local descriptor learning loss (2018)
15. Moosmann, F., Stiller, C.: Velodyne slam. In: 2011 IEEE Intelligent Vehicles Symposium (IV). pp. 393–398 (2011). <https://doi.org/10.1109/IVS.2011.5940396>
16. Mur-Artal, R., Tardós, J.D.: Orb-slam2: An open-source slam system for monocular, stereo, and rgb-d cameras. *IEEE transactions on robotics* **33**(5), 1255–1262 (2017)
17. Ronneberger, O., Fischer, P., Brox, T.: U-net: Convolutional networks for biomedical image segmentation (2015)
18. Schmid, J.F., Simon, S.F., Mester, R.: Features for ground texture based localization—a survey. *arXiv preprint arXiv:2002.11948* (2020)
19. Schmid, J.F., Simon, S.F., Mester, R.: Ground texture based localization using compact binary descriptors. In: 2020 IEEE International Conference on Robotics and Automation, ICRA 2020, Paris, France, May 31 - August 31, 2020. pp. 1315–1321. IEEE (2020). <https://doi.org/10.1109/ICRA40945.2020.9197221>, <https://doi.org/10.1109/ICRA40945.2020.9197221>
20. Teja, P.R., Kumaar, A.A.N.: Qr code based path planning for warehouse management robot. In: 2018 International Conference on Advances in Computing, Communications and Informatics (ICACCI). pp. 1239–1244 (2018). <https://doi.org/10.1109/ICACCI.2018.8554760>
21. Wang, X., Han, X., Huang, W., Dong, D., Scott, M.R.: Multi-similarity loss with general pair weighting for deep metric learning. In: IEEE Conference on Computer Vision and Pattern Recognition, CVPR 2019, Long Beach, CA, USA, June 16–20, 2019. pp. 5022–5030. Computer Vision Foundation / IEEE (2019). <https://doi.org/10.1109/CVPR.2019.00516>
22. Wu, K., Otoo, E., Shoshani, A.: Optimizing connected component labeling algorithms. In: Medical Imaging 2005: Image Processing. vol. 5747, pp. 1965–1976. International Society for Optics and Photonics (2005)
23. Zhang, H., Zhang, C., Yang, W., Chen, C.Y.: Localization and navigation using qr code for mobile robot in indoor environment. In: 2015 IEEE International Conference on Robotics and Biomimetics (ROBIO). pp. 2501–2506 (2015). <https://doi.org/10.1109/ROBIO.2015.7419715>
24. Zhang, L., Finkelstein, A., Rusinkiewicz, S.: High-precision localization using ground texture. In: 2019 International Conference on Robotics and Automation (ICRA). pp. 6381–6387. IEEE (2019)
25. Zhang, L., Rusinkiewicz, S.: Learning to detect features in texture images. In: Proceedings of the IEEE conference on computer vision and pattern recognition. pp. 6325–6333 (2018)
26. Zheng, L., Yang, Y., Tian, Q.: Sift meets cnn: A decade survey of instance retrieval. *IEEE Transactions on Pattern Analysis and Machine Intelligence* **40**(5), 1224–1244 (2018). <https://doi.org/10.1109/TPAMI.2017.2709749>